Visual Odometry and Low Optic Flow Measurement by Means of a Vibrating Artificial Compound Eye

Fabien Colonnier, Augustin Manecy, Raphaël Juston, and Stéphane Viollet(✉)

Aix-Marseille Université, CNRS, ISM UMR 7287, 13288 Marseille Cedex 09, France
stephane.viollet@univ-amu.fr
http://www.biorobotics.eu

Abstract. In this study, a tiny artificial compound eye (diameter 15mm) named CurvACE (which stands for Curved Artificial Compound Eye), was endowed with hyperacuity, based on an active visual process inspired by the retinal micro-movements occurring in the fly's compound eye. A periodic (1-D, 50-Hz) micro-scanning movement with a range of a few degrees (5°) enables the active CurvACE to locate contrasting objects with a 40-fold greater accuracy which was restricted by the narrow interommatidial angle of about 4.2°. This local hyperacuity was extended to a large number of adjacent ommatidia in a novel visual processing algorithm, which merges the output signals of the local processing units running in parallel on a tiny, cheap micro-controller requiring very few computational resources. Tests performed in a textured (indoor) or natural (outdoor) environment showed that the active compound eye serves as a contactless angular position sensing device, which is able to assess its angular position relative to the visual environment. As a consequence, the vibrating compound eye is able to measure very low rotational optic flow up to $20^\circ/s$ and perform a short range odometry knowing the altitude, which are two tasks of great interest for robotic applications.

Keywords: Hyperacuity · Robotics · Eye micro-movements · Insect vision

1 Introduction

The curved compound eye depicted in the present study is the first example of an artificial compound eye which is able to locate targets or determine its orientation relative to the visual environment, with a much greater accuracy than the one imposed by its optics (i.e. by the interommatidial and acceptance angles). Findings on the visual processes at work in the fly inspired us to design and construct an active version of the previously described cylindrical compound eye CurvACE, which was based on an array of artificial ommatidia [4] and [12]. This active compound eye features two properties that are usually banned by

S.P. Wilson et al. (Eds.): Living Machines 2015, LNAI 9222, pp. 153–163, 2015.
DOI: 10.1007/978-3-319-22979-9_16

optic sensor designers because they detract from the sharpness of the resulting images: optical blurring and vibration. The first micro-scanning sensor based on the periodic retinal micro-movements observed in the fly (for a review, see [11]) was presented in [9]. This scanning eye was capable of detecting low levels of translational optic flow, such as those encountered by a mobile robot around its heading direction (the focus of expansion).

In the present study, hyperacuity was based on the existence of an overlap between the receptive visual fields of 2 neighbouring ommatidia. In a fly's ommatidium, each photoreceptor has a quasi-Gaussian ASF (Angular Sensitivity Function), which is given by the convolution of the point spread function of the facet lens with the photoreceptors diameter [5] - [10].

An artificial curved compound eye can provide a useful optic flow measurement and motion detection ability (see [4]). Moreover, we established here that the same compound eye subjected to active periodic micro-scanning movements combined with appropriate visual processing algorithms can be endowed with angular position sensing abilities.

Brückner et al. assessed the hyperacuity of an artificial compound eye in terms of its ability to locate a point source or an edge [1]. The robustness of these visual sensors' performances with respect to the contrast and the distance from the object targeted has not been addressed so far, however. In our previous paper [2], we report that the active CurvACE enabled a robot to perform visual odometry and track a target moving over a textured ground. These two properties are of great interest for designing autonomous robotic aerial vehicles. Section 2 describes the active version of the CurvACE eye inspired from the fly's retinal micro-movements. A complete description of the visual processing algorithms resulting in hyperacuity is presented in section 3, and section 4 describes the ability of the active CurvACE to assess its angular orientation and speed based on the novel sensory fusion algorithm developed here. Another application shows that this measurement can also be used in a linear positioning task, relatively to the environment.

2 Eye Movements Inspired by the Fly's Visual Micro-scanning Movements

In this study, visual hyperacuity results from an active process whereby periodic micro-movements are continuously applied to an artificial compound eye. This approach was inspired by the retinal micro-movements observed in the eye of the blowfly *Calliphora*. Unlike the fly's retinal scanning movements, which result from the translation of the photoreceptors in the focal plane of each individual facet lens (for a review on the fly's retinal micro-movements see [11]), the eye tremor applied here to the active CurvACE by means of a micro-stepper motor (figure 1) results from a periodic rotation of the whole artificial compound eye.

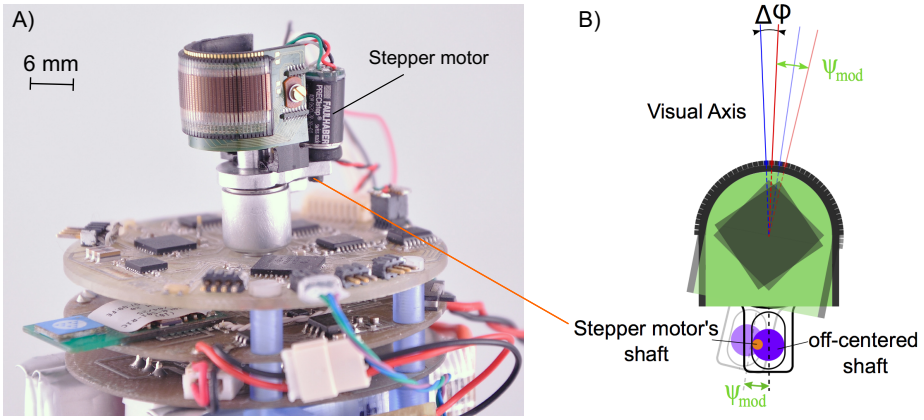

Fig. 1. Artificial vibrating compound eye. A) Active CurVACE sensor with its vibrating mechanism based on the use of a tiny stepper motor. A small periodic movement is applied to the artificial CurvACE compound eye composed of 630 ommatidia, which has a diameter of only 15 mm, giving a panoramic horizontal FOV of 180° and a vertical FOV of 60° (see [4] for details). B) Diagram of the micro-scanning compound eye subjected to active periodic rotational movements generated by a miniature eccentric mechanism. The angular vibration ψ_{mod} is generated by the miniature stepper motor shown here in the form of an orange shaft and a purple off-centered shaft, which translates along the oblong hole. The scanning frequency can be easily adjusted by changing the rotational speed of the motor. The scanning amplitude depends on the offset between the motor shaft and the off-centered shaft.

3 Insights Into the Visual Processing Algorithm

3.1 Edge and Bar Location by an Active Compound Eye

As shown in figure 2, each local processing unit (LPU) is connected to a pair of adjacent ommatidia. For further details about the implementation and characterization of the LPU, see [7] and [6].

One LPU's output signal results from the difference-to-sum ratio of the demodulated photoreceptor signals, as follows:

$$Output_{Pos} = \frac{Ph_{1demod} - Ph_{2demod}}{Ph_{1demod} + Ph_{2demod}} \tag{1}$$

Equation (1) in the original model for the VODKA sensor [7] placed in front of an edge can be greatly simplified as follows:

$$\theta_i(\Psi_c) = K_1 \cdot tanh\left(\frac{4\Delta\varphi log(2)}{\Delta\rho^2}\Psi_c\right) \tag{2}$$

with θ_i the output signal of an LPU (see figure 2). Due to the limited FOV of each LPU, the angular position θ_i of a contrasting object ranges from $-2°$ to $2°$.

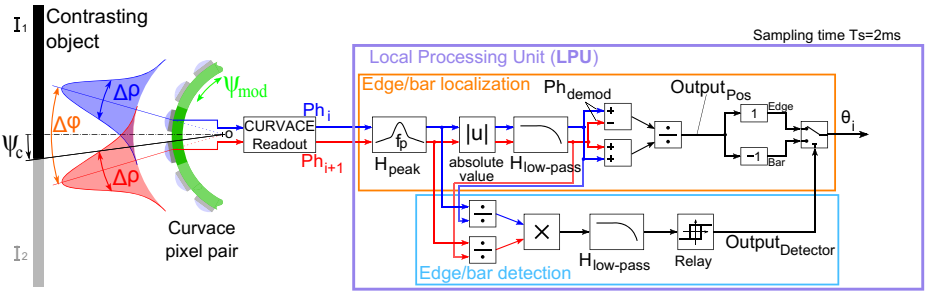

Fig. 2. Block diagram of the elementary local processing unit (LPU) integrated into the active Curvace for locating edges and bars with great accuracy. The stepper motor (see figures 1) generates a periodic rotation $\psi_{mod}(t)$ (green double arrows) of the overall compound eye, resulting in the angular microscanning of their visual axes, in keeping with a sinusoidal law (scanning frequency 50Hz, amplitude about 5° peak to peak with $\Delta\varphi = 4.2°$ and $\Delta\rho = 4.2°$). Two parallel processing pathways (one for edge/bar localization and one for edge/bar detection) were implemented. The edge/bar localization block gives the local angular position θ_i of an edge or bar placed in the visual field of two adjacent ommatidia. The edge/bar detection block detects the presence of a bar or edge and triggers the appropriate sign: +1 for edges and -1 for bars. The principle of this detector is described in [6]. The central frequency f_p of the peak filter is equal to the scanning frequency (50Hz), whereas the cut-off frequency of the second order digital low-pass filter is equal to 10Hz. Adapted from [6].

The photoreceptor output signals (Ph_i and Ph_{i+1}) were first digitized by means of a 10-bit analog-to-digital converter integrated into each column of the CurvACE eye (see [4] for further details). A peak filter acts as both a differentiator and a selective filter centered at the scanning frequency ($f_p = f_{mod}$). The classical amplitude demodulation procedure used here was based on an absolute value function cascaded with a low-pass filter to smooth out the photoreceptor's output signals. Arithmetic operations were performed to obtain the sensor's output signal, as described in [7] - [6]. An innovative edge/bar detector was also included and used to select the sign of the $Output_{Pos}$ (see [6] for further details about the Edge/bar detection process).

3.2 Hyperacute Localization of Contrasting Bars and Edges

The characteristic static curve of the active CurvACE obtained with a contrasting edge and a black bar 1cm in width subtending an angle of 2.8° is presented in figure 3.

As was to be expected in view of equation (2), the curve in figure 3a has a tangent hyperbolic profile with respect to the angular position of the edge. It can be clearly seen by comparing the two curves plotted in figure 3 that the slopes of the characteristic static curves obtained with a bar and an edge are inverted. A theoretical explanation for this inversion of the slopes is given in

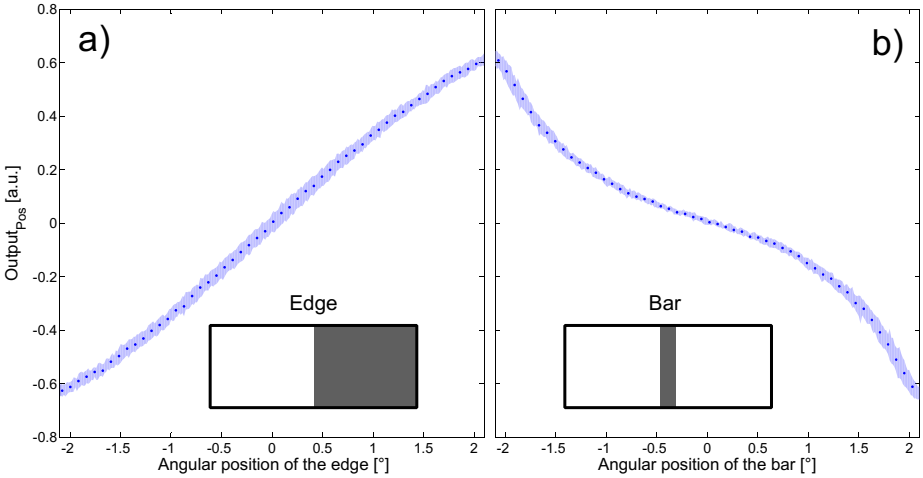

Fig. 3. Characteristic static curves of one LPU (see figure 2). The $Output_{Pos}$ signal is plotted versus the angular position of a) an edge or b) a bar placed 20 cm in front of active CurvACE rotating in 0.075° steps, each lasting 0.5s. It can be clearly seen from this figure that the slope of the characteristic static curve obtained with a bar is inverted in comparison with that obtained with an edge. Bars therefore have to be distinguished from edges in order to select the appropriate sign of the gain K (see figure 2). Adapted from [2].

[6]. This inversion fully justifies the use of an edge/bar detector (see figure 2) to compensate for the gain inversion.

3.3 Merging the Output of Local Pairs of Processing Units

To endow a robot with the capability to sense its angular speed and position, a novel sensory fusion algorithm was developed using several LPU in parallel. An example of implementation shows in figure 4 a 2D region of interest (ROI) composed of 8×5 artificial ommatidia. The algorithm used here implements the connection between the 8×5 photosensors' output signals to an array of 7×5 LPUs in order to provide local measurements of edge and bar angular positions. Then, a selection is performed by computing the local sum S of two demodulated signals Ph_{demod} obtained from two adjacent photosensors:

$$S_{n,n+1} = Ph_{(n)_{demod}} + Ph_{(n+1)_{demod}} \tag{3}$$

Indeed, as a signal $Output_{Pos}$ is pure noise when no feature is in the field of view, an indicator of the presence of a contrast was required. The sum of the demodulated signals was used here to give this feedback, because we observed that the contrast is positively correlated with the sum and the Signal-to-Noise Ratio. Therefore, at each sampling step, each local sum S is thresholded in order to select the best LPU's outputs to use. All the sums above the threshold value

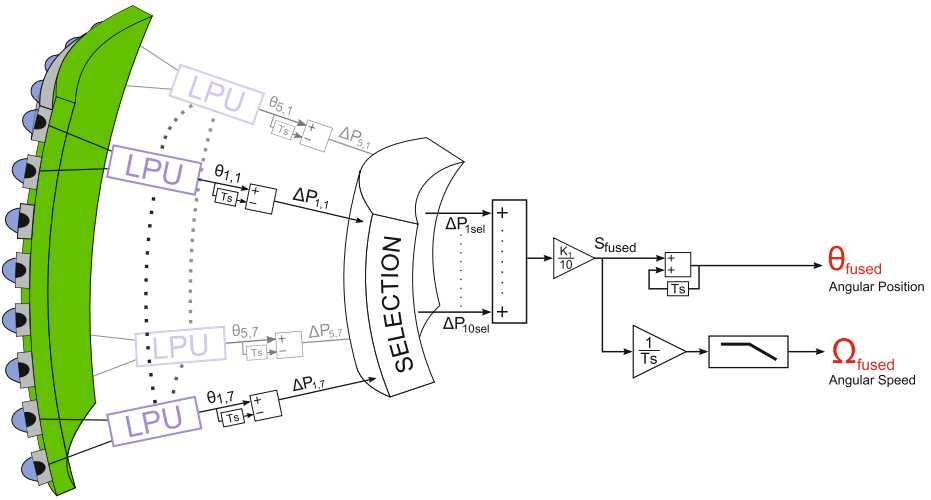

Fig. 4. Description of the sensory fusion algorithm to assess the angular speed Ω_{fused} as well as the position θ_{fused} resulting here from a translation of the textured panel with respect to the arbitrary reference position (i.e. the initial position if not resetting during the experiment). The 35 (7×5) LPU output signals corresponding to the ROI (8×5 photosensors) of the active CurvACE were processed by the 35 Local Processing Units (LPUs) presented in figure 2. Here, the signal obtained before reaching the discrete integrator, denoted S_{fused}, was used to compute the angular speed. This procedure involved normalizing the time $\frac{1}{T_s}$, with T_s equal to the sample time of the system. A first order low-pass filter with a cut-off frequency of $1.6Hz$ limited the noise. The sensor's position θ_{fused} was scaled in degrees by means of the gain K_1. Adapted from [2].

are kept and the others are rejected. The threshold is then increased or decreased by a certain amount until 10 local sums have been selected. The threshold therefore evolves dynamically at each sampling time step. Lastly, the index i of each selected sum S gives the index of the pixel pair to process. Thus, the computational burden is dramatically reduced. Moreover, this selection helps to reduce the data processing because only the data provided by the 10 selected LPUs are actually processed by the micro-controller.

In a nutshell, the sensory fusion algorithm presented here selects the 10 highest contrasts available in the FOV. As a result, the active CurvACE is able to assess its relative linear position regarding its initial one and its speed with respect to the visual environment.

It is worth noting that the selection process acts like a strong non-linearity. The output signal θ_{fused} is therefore not directly equal to the sum of all the local angular positions θ_i. The parallel differentiation coupled to a single integrator via a non-linear selecting function merges all the local angular positions θ_i, giving a reliable measurement of the angular orientation of the visual sensor within an infinite range. The active CurvACE can therefore be said to serve as a visual

compass once it has been subjected to a rotational movement (see section 5). Mathematically, the position is given through the 3 equations as follows:

$$\begin{cases} \Delta P_{i_{sel}} = \theta_{i_{sel}}(t) - \theta_{i_{sel}}(t-1) \\ \theta_{fused}(t) = \theta_{fused}(t-1) + \dfrac{K_1}{10} \displaystyle\sum_{i=1}^{10} \Delta P_{i_{sel}} \\ \Omega_{fused}(t) = \dfrac{1}{Ts}(\theta_{fused}(t) - \theta_{fused}(t-1)) \end{cases} \tag{4}$$

As shown in figure 4, the eye's speed is determined by applying a low-pass filter to the fused output signal S_{fused} (which is the normalized sum of the local displacement error ΔP_{isel}), whereas the eye's position is determined in the same way as θ_{fused}, with the gain K_1 (equal to 3.814).

To sum up, the algorithm developed here sums the local variation of contrast angular positions in the sensor field of view to be able to give the angular displacement.

4 Experimental Results

4.1 Measurement of Very Low Optic Flow

In optic flow based navigation, the measurement of very low angular speed can be crucial, for example, to compensate for very low drift or to measure the translational optic flow values near the focus of expansion, which is by essence very low. We characterized here our vibrating compound eye outdoors by making the eye rotate at variable speed ranging from 0 to $20°/s$. The ROI was a single line composed of 42 ommatidia leading to a visual field of 180°. Figure 5 shows that the angular position and speed are well measured by the sensor. Even if the speed is relatively noisy because of the derivative process, it still can be used as a feedback in a control loop, as demonstrated in [2]. It is worth noting that the range of rotational optic flow that can be measured by active CurvACE is very complementary to the one measured by bio-inspired optic flow sensors. For a similar outdoor environment, the optic flow sensors were able to measure variations from $50°/s$ to $300°/s$ (see [3] for further details). As a consequence, activating the periodic micro-eye movements can enhance largely the eye's motion sensing sensitivity to detect very slow movements such as those occurring near the poles of the optic flow field or resulting from a slow drift.

4.2 Short Range Visual Odometry

In the previous experiment (see figure 5), the FOV was composed of one complete CurvACE line (consisting of 42 ommatidia). Here we focus on a FOV composed of 40 ommatidia, but organized in a ROI of 8 by 5 ommatidia (giving a FOV of about 32° by 20°).

By placing infrared reflective markers on a rotating arm supporting the active CurvACE, it was possible to measure with great accuracy the ground truth

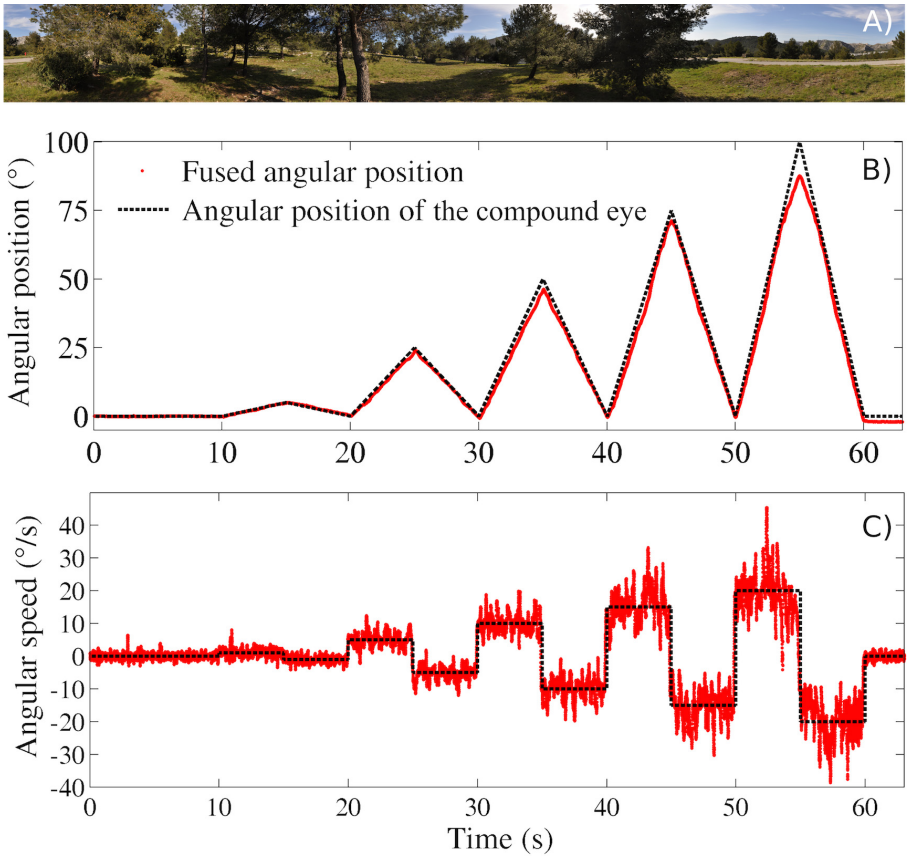

Fig. 5. Measured static characteristics of the active CurvACE placed outdoors in a natural environment (A). B) Fused output signals θ_{fused} superimposed with the angular position of the active CurvACE. The latter can be seen to have served here as a visual compass giving its relative angular position with respect to the environment. C) Eye's rotational speed calculated from B) by applying a discrete derivative the eye's angular position. The eye can provide a good estimation of its angular speed and thus the rotational optic flow even at very low speed ranging from 0 to $20°/s$.

position (curvilinear abscissa) of the eye, which can be compared with the active CurvACE's visual output signal. Once the active CurvACE's output signal has been calibrated, it can be used directly to give the linear position of the eye with respect to the visual environment (a textured panel) placed 39cm below the eye. All the signal processing algorithms have been entirely implemented onboard an electronic board based on a 16-bit microcontroller (dSPic from Microchip) connected to the eye.

The eye's output signal θ_{fused}, which was scaled in millimetres, assuming the height to be known, is superimposed in Figure 6 on the absolute (ground truth)

position of the eye measured by the VICON system. The excellent accuracy of the linear position measurement given by the active CURVACE makes it a good candidate for stabilizing an aerial robot when it is flying over an arbitrary terrain (see [2]).

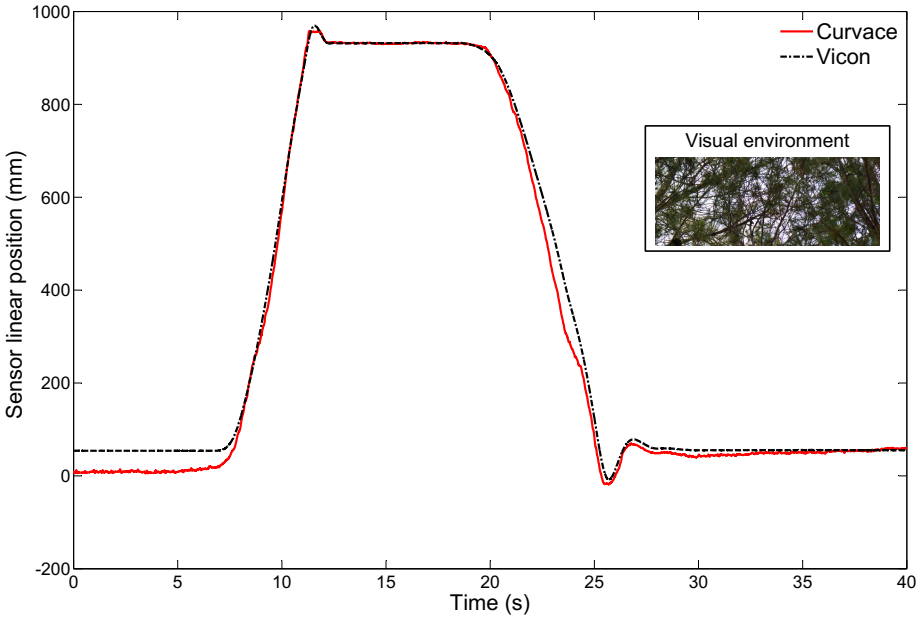

Fig. 6. The active CurvACEs output signal (red) superimposed on the linear position of the eye (dashed black) measured by the VICON system. The good match observed between the two curves shows that the vibrating compound eye can be served as a visual odometer during short range displacements over landscapes such as the textured 2-D pattern composed of branches and leaves tested here.

5 Conclusion

In this paper, we describe the development and the characterization of the active version of a tiny cylindrical curved compound eye named CurvACE. The active process referred to here means that miniature periodic eye movements have been added in order to improve CurvACE's perception of the environment in terms of the localization of the contrasting objects encountered. By subjecting this artificial compound eye to oscillatory movements (micro-scanning movements with a frequency of 50Hz) with an amplitude of a few degrees (5°), it was endowed with hyperacuity, i.e., the ability to *locate* an object with a much greater accuracy than that which was possible so far because of the restrictions imposed

by the interommatidial angle. Hyperacuity was achieved here by several (41 or 35, depending on the experiment) local processing units applying the same local visual processing algorithm across a ROI of active CurvACE sensors, each of which was connected to a pair of adjacent ommatidia. The novel sensory fusion algorithm used for this purpose, which was based on the selection of the 10 highest contrasts, enables the active eye to assess its relative angular orientation (1D-FOV: 180° by 4°) or its linear position (2D-FOV : 32° by 20°) with respect to natural or textured environments. All the solutions adopted in this study in terms of practical hardware and computational resources are perfectly compatible with the stringent specifications of very low power consumption, small size and low cost micro-aerial vehicles (MAVs). Moreover, the MAV of the future (e.g. [8]) will certainly require very few computational resources to perform demanding tasks such as automatic navigation, obstacle avoidance and visual stabilization. By applying miniature eye movements to a stand-alone artificial compound eye, we obtained a reliable visual compass when the active eye was subjected to purely rotational movements, and a visual odometer when it was subjected to purely translational movements (see also [2]). These two fundamental features will certainly be of great value in various fields of research, from metrology to robotics.

Acknowledgments. The authors would like to thank Marc Boyron and Julien Diperi for the robot and the test bench realization; Nicolas Franceschini for helping in the design of the robot, Franck Ruffier for the fruitful discussions and the help for implementing the flying arena. We also acknowledge the financial support of the Future and Emerging Technologies (FET) program within the Seventh Framework Programme for Research of the European Commission, under FET-Open Grant 237940. This work was supported by CNRS, Aix-Marseille University, Provence-Alpes-Cote d'Azur region and the French National Research Agency (ANR) with the EVA, IRIS and Equipex/Robotex projects (EVA project and IRIS project under ANR grants' number ANR608-CORD-007-04 and ANR-12-INSE-0009, respectively).

References

1. Brückner, A., Duparré, J., Bräuer, A., Tünnermann, A.: Artificial compound eye applying hyperacuity. Opt. Express **14**(25), 12076–12084 (2006). http://www.opticsexpress.org/abstract.cfm?URI=oe-14-25-12076
2. Colonnier, F., Manecy, A., Juston, R., Mallot, H., Leitel, R., Floreano, D., Viollet, S.: A small-scale hyperacute compound eye featuring active eye tremor: application to visual stabilization, target tracking, and short-range odometry. Bioinspiration & Biomimetics **10**(2), 026002 (2015). http://stacks.iop.org/1748-3190/10/i=2/a=026002
3. Expert, F., Viollet, S., Ruffier, F.: Outdoor field performances of insectbased visual motion sensors. Journal of Field Robotics **28**, 529–541 (2011)
4. Floreano, D., Pericet-Camara, R., Viollet, S., Ruffier, F., Brckner, A., Leitel, R., Buss, W., Menouni, M., Expert, F., Juston, R., Dobrzynski, M., L'Eplattenier, G., Recktenwald, F., Mallot, H., Franceschini, N.: Miniature curved artificial compound eyes. Proc. Natl. Acad. Sci. USA **110**(23), 9267–9272 (2013). http://dx.doi.org/10.1073/pnas.1219068110

5. Franceschini, N., Chagneux, R.: Repetitive scanning in the fly compound eye. In: Göttingen Neurobiology Report, vol. 2. Thieme (1997)
6. Juston, R., Kerhuel, L., Franceschini, N., Viollet, S.: Hyperacute edge and bar detection in a bioinspired optical position sensing device. IEEE/ASME Transactions on Mechatronics **PP**(99), 1–10 (2013)
7. Kerhuel, L., Viollet, S., Franceschini, N.: The vodka sensor: A bio-inspired hyperacute optical position sensing device. IEEE J. Sensor **12**(2), 315–324 (2012). http://www.sciencemag.org/content/340/6132/603.abstract
8. Ma, K.Y., Chirarattananon, P., Fuller, S.B., Wood, R.J.: Controlled flight of a biologically inspired, insect-scale robot. Science **340**(6132), 603–607 (2013)
9. Mura, F., Franceschini, N.: Obstacle avoidance in a terrestrial mobile robot provided with a scanning retina. In: Proc. IEEE Intelligent Vehicles Symposium, pp. 47–52, September 19–20, 1996
10. Stavenga, D.G.: Angular and spectral sensitivity of fly photoreceptors. i. integrated facet lens and rhabdomere optics. J. Comp. Physiol. A, Neuroethol. Sens. Neural. Behav. Physiol. **189**(1), 1–17 (2003). http://dx.doi.org/10.1007/s00359-002-0370-2
11. Viollet, S.: Vibrating makes for better seeing: from the flys retinal micro-movements to hyperacute bio-inspired visual sensors. Frontiers in Bionics and Biomimetics (submitted 2014)
12. Viollet, S., Godiot, S., Leitel, R., Buss, W., Breugnon, P., Menouni, M., Juston, R., Expert, F., Colonnier, F., L'Eplattenier, G., Brückner, A., Kraze, F., Mallot, H., Franceschini, N., Pericet-Camara, R., Ruffier, F., Floreano, D.: Hardware architecture and cutting-edge assembly process of a tiny curved compound eye. Sensors **14**(11), 21702–21721 (2014). http://www.mdpi.com/1424-8220/14/11/21702